CHEMISTRY & BIODIVERSITY

Accepted Article

Title: Synthesis, molecular docking and preliminary antileukemic activity of 4-methoxybenzyl derivatives bearing an imidazo[2,1-b][1,3,4]thiadiazoles

Authors: Subhas S. Karki, B Choodamani, Karla G Cano Hernandez, Sujeet Kumar, Anna M Tony, Austre Y Schiaffino Bustamante, Renato J Aguilera, Dominique Schols, and GopiMohan Gopi C

To be cited as: *Chem. Biodiversity* 10.1002/cbdv.202000800

Link to VoR: https://doi.org/10.1002/cbdv.202000800

10.1002/cbdv.202000800

Synthesis, molecular docking and preliminary antileukemic activity of 4-methoxybenzyl derivatives bearing an imidazo[2,1-*b*][1,3,4]thiadiazoles

Chudamani B,[a,b*] Karla G. Cano Hernandez,[c*] Sujeet Kumar,[a] Ann Maria Tony,[d] Austre Y. Schiaffino Bustamante,[c] Renato J. Aguilera,[c] Dominique Schols,[e] C Gopi Mohan,[d] Subhas S. Karki[a,b**]

[a]Department of Pharmaceutical Chemistry, KLE College of Pharmacy, (A Constituent Unit of KAHER-Belagavi) Bengaluru, 560010, Karnataka, India
[b]Dr. Prabhakar B. Kore Basic Science Research Center, Off-Campus, KLE College of Pharmacy, (A Constituent Unit of KAHER-Belagavi) Bengaluru, 560010, Karnataka, India
[c]The Cellular Characterization and Biorepository Core Facility & Border Biomedical Research Center& Department of Biological Sciences, The University of Texas at El Paso, El Paso, 79968 TX, USA
[d]Centre for Nanosciences and Molecular Medicine, Amrita Institute of Medical Sciences and Research Centre, Amrita Vishwa Vidyapeetham, Kochi, 682041, Kerala, India
[e]Rega Institute for Medical Research, Department of Microbiology, Immunology and Transplantation, Laboratory of Virology and Chemotherapy, KU Leuven, B-3000 Leuven, Belgium

*Equal first author

**Corresponding author: +91 8023325611 (Off); +91 8023425373 (fax);

subhasskarki@gmail.com (Subhas S Karki)

10.1002/cbdv.202000800

A B S T R A C T

In this study, we synthesized 22 compounds in a series with various substitution on imidazo[2,1-*b*][1,3,4]thiadiazoles. The potential cytotoxic activity of these compounds investigated in leukemia cell lines by Differential Nuclear Staining (DNS). Our results identify two compounds 2-(4-methoxybenzyl)-6-(2-oxo-2H-chromen-3-yl)imidazo[2,1-b][1,3,4]thiadiazol-5-yl thiocyanate and 6-(4-chlorophenyl)-2-(4'-methoxybenzyl)imidazo[2,1-b][1,3,4]thiadiazole-5-carbaldehyde exhibited as the most cytotoxic effect against murine leukemia cells (L1210), human T-lymphocyte cells (CEM) and human cervix carcinoma cells (HeLa) with IC_{50} values ranging between 0.79 to 1.6 μM. The results indicate that compound 2-(4-methoxybenzyl)-6-(2-oxo-2H-chromen-3-yl)imidazo[2,1-b][1,3,4]thiadiazol-5-yl thiocyanate is inducing phosphatidylserine externalization and caspase-3 activation which are both a hallmark of apoptosis. Docking studies showed that compound 2-(4-methoxybenzyl)-6-(2-oxo-2H-chromen-3-yl)imidazo[2,1-b][1,3,4]thiadiazol-5-yl thiocyanate binds within the active sites of transforming growth factor beta (TGF-**β)** type I receptor kinase domain by strong hydrogen binding and hydrophobic interactions.

Keywords: Imidazothiadiazole, Cytotoxicity, TGF beta receptor kinase, Melphalan, Levamisole

Introduction

According to the American Cancer Society, in the United States, by 2020, more than 60,000 new cases of leukemia are expected to be diagnosed. This year leukemia is expected to cause around 20,000 deaths.[1] Leukemia is a type of cancer characterized by uncontrolled proliferation of hematopoietic stem cells in the bone marrow.[2] There are multiple types of leukemia often grouped in acute leukemia, when cancer can progress rapidly and chronic leukemia that refers to slower progression.[3] Furthermore, leukemia is divided on the type of bone marrow cell where cancer starts. Lymphoblastic leukemia is the other type, which is characterized by starting in cells that would regularly become lymphocytes.[4] Combining these grouping criteria, there are 4 main types of leukemia that are; chronic lymphocytic leukemia, chronic myeloid leukemia, acute lymphocytic leukemia, and acute myeloid leukemia.[4] The development of treatments for leukemia has advanced over the years. The main type of treatment given to patients is chemotherapy includes drugs, such as, vincristine, daunorubicin, and cytarabine.[5] The improvements in leukemia treatments has increased the 5-year survival rate to 63%.[6] However, the development of more effective treatments is needed to decrease the number of fatalities caused by this disease.

Levamisole (I) was approved by the FDA in 1990 as a curative treatment for colon cancer.[7] Prior to this, levamisole was used as an antirheumatic treatment in the 1970s and 1980s in patients with rheumatoid arthritis.[8] Due to the protective effects of the immune system, the drug has been studied in the treatment of various immune-mediated diseases, and some studies have shown positive effects.[9] The drug has also been used in combination with other drugs to treat various cancers.[8.9] In 1982, a clinical trial revealed that in acute myeloid leukemia patients the combination of levamisole with 6-mercaptopurine and methotrexate resulted in better remission of cancer, compared to those given only the chemotherapy.[10]

Transforming growth factor (TGF β) is a cytokine, which plays a key role in cell proliferation, differentiation and apoptosis.[11] TGF β type 1 is activin receptor-like kinase 5

10.1002/cbdv.202000800

(ALK5) and plays a key role in TGF β signaling pathway. ALK5 receptor promotes angiogenesis.[12] Various small molecules such as GW6604 (**II**),[13] galunisertib (LY-2157299)[14] (**III**) imidazo[2,1-*b*],1,3,4]thiadiazole[15,16] (**IV**) as ALK5 inhibitors. Our group reported cytotoxic activity of different imidazo[2,1-*b*][1,3,4]thiadiazole.[17-24] Considering the importance of imidazothiadiazole fused ring, we prepared twenty two compounds of 2-(4-methoxybenzyl)-imidazo[2,1-*b*][1,3,4]thiadiazole (**V**) as cytotoxic by bringing phosphatidylserine externalization activity, which is a hallmark of apoptosis and binds within the active sites of the TGF β receptor kinase (**Figure 1**).

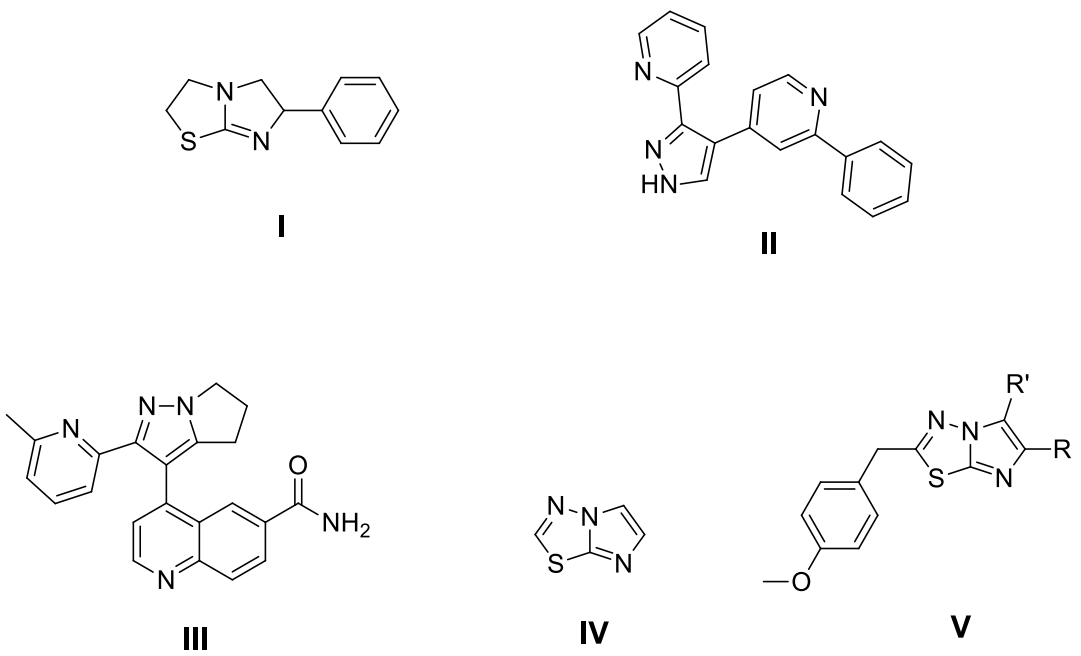

Figure 1. Structures of various (fused) heterocyclic compounds (**I-IV**) as anticancer and inhibitors of ALK 5 and synthesized cytotoxic compounds (**V**).

Results and Discussion

Chemistry

5-(4-methoxybenzyl)-1,3,4-thiadiazole-2-amine (**3**) was obtained by reacting 4-methoxyphenyl acetic acid (**1**) and thiosemicarbazide (**2**) in sulfuric acid at 60-70 ºC for 8 h and made alkaline with ammonia solution. Various 6-aryl substituted 2-(4-methoxybenzyl)-imidazo[2,1-

b][1,3,4]thiadiazoles (**5a-h**) obtained by reacting **3** with various 2-bromo ketones (**4**) in alcohol by refluxing in ethyl alcohol for 12 h and neutralizing with aqueous sodium carbonate. The expected 5-substituted derivatives **6a-e, 7a-g** and **8a, 8b** was prepared by electrophilic substitution on imidazo[2,1-*b*][1,3,4]thiadiazoles **5a-h** (**Scheme 1**).

Scheme 1 Synthetic pathway of 2-(4-methoxybenzyl)-6-aryl-imidazo[2,1-*b*][1,3,4]-thiadiazole.

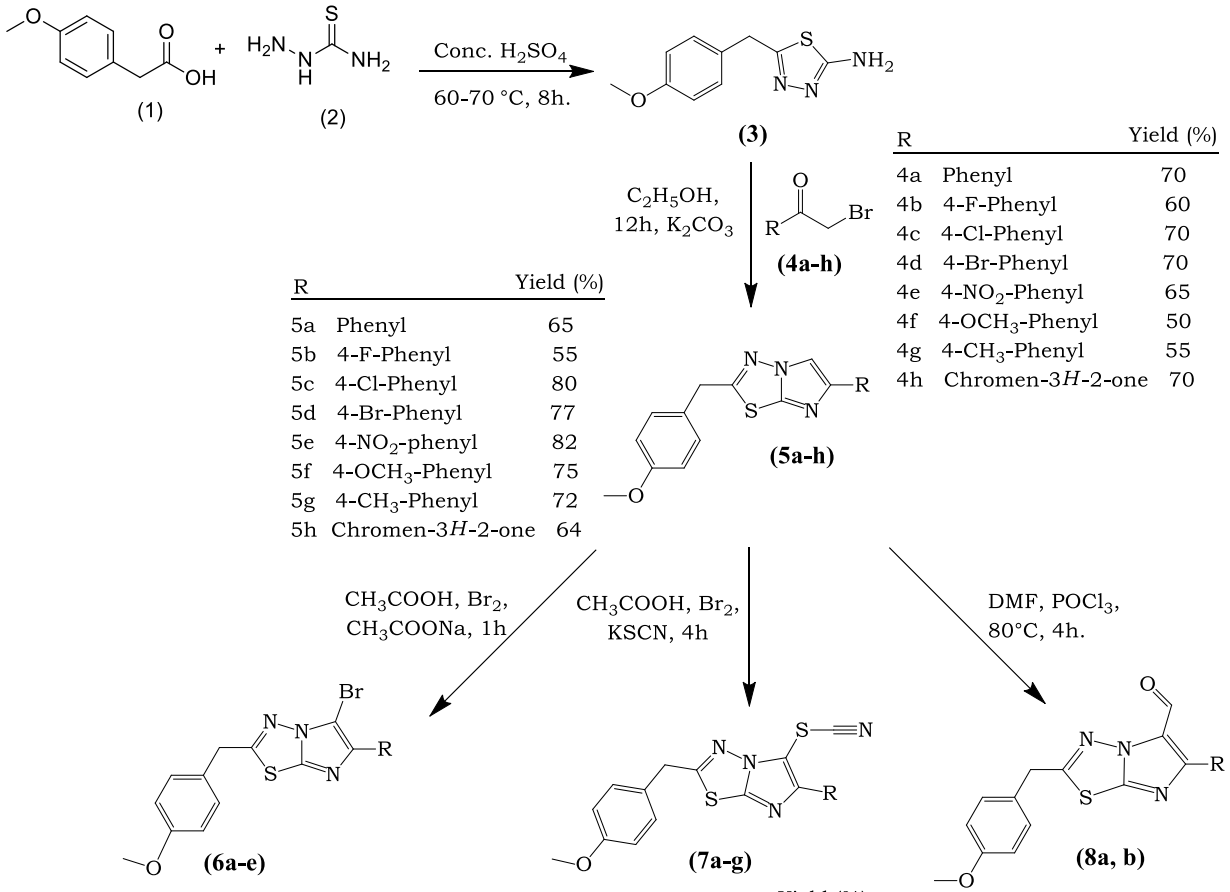

R		Yield (%)
4a	Phenyl	70
4b	4-F-Phenyl	60
4c	4-Cl-Phenyl	70
4d	4-Br-Phenyl	70
4e	4-NO_2-Phenyl	65
4f	4-OCH_3-Phenyl	50
4g	4-CH_3-Phenyl	55
4h	Chromen-3*H*-2-one	70

R		Yield (%)
5a	Phenyl	65
5b	4-F-Phenyl	55
5c	4-Cl-Phenyl	80
5d	4-Br-Phenyl	77
5e	4-NO_2-phenyl	82
5f	4-OCH_3-Phenyl	75
5g	4-CH_3-Phenyl	72
5h	Chromen-3*H*-2-one	64

R		Yield (%)
6a	Phenyl	60
6b	4-F-Phenyl	58
6c	4-Cl-Phenyl	63
6d	4-Br-Phenyl	55
6e	4-CH_3-Phenyl	58

R		Yield (%)
7a	Phenyl	70
7b	4-F-Phenyl	65
7c	4-Cl-Phenyl	60
7d	4-Br-Phenyl	75
7e	4-OCH_3-Phenyl	65
7f	4-CH_3-Phenyl	74
7g	Chromen-3*H*-2-one	66

R		Yield (%)
8a	Phenyl	55
8b	4-Cl-Phenyl	60

The structures of the newly prepared compounds have been confirmed on the bases spectroscopic data (^{1}H-NMR, ^{13}C-NMR, HRMS and FTIR). Fourier transform infra-red (FTIR) spectroscopy of the synthesized compounds **(5a-8b)** showed characteristic vibrations between 3172-3006 cm^{-1} for C-H stretching, 2987-2750 cm^{-1} for C-H aliphatic stretching. In addition, the compounds **5h** and **7g** showed vibrations between 1710-1668 cm^{-1} for carbonyl stretching. While for the compounds (**7a-g)** containing -C≡N functional group exhibited infrared vibrations between 2171-2163 cm^{-1}. In ^{1}H NMR, the imidazole proton (C_5-H) appeared between 8.91-8.48 δ ppm and that confirms the reaction of 2-amino-5-(4-methoxybenzyl)-1,3,4-thiadiazole (**3**) with respective 2-bromoketone (**4**). The absence of hydrogen at C_5 position of imidazothiadiazole nucleus confirms the substitution at C_5 position. A singlet observed between 10.00 and 9.98 δ ppm for the compounds **8a** and **8b** confirmed for the introduction of the formyl group by Vilsmeier-Haack reaction. Aromatic protons appeared as multiplet signals between 8.02-6.94 δ ppm. Bridge headed -CH_2- proton (at C_2) exhibited as a singlet between 4.50-4.34 δ ppm for all compounds. The presence of methoxy proton for all the compounds observed between 3.84-3.74 δ ppm as a singlet. Compounds having CH_3 **(5g, 6e & 7f**) proton appeared from 2.37-2.30 δ ppm as a singlet. The HR-MS spectrum of the newly synthesized compounds showed their molecular ion peak with their respective molecular weights and therefore confirms for the authenticity of the all compounds. Refer **Scheme 1** for the details of the synthesized compounds.

Cytotoxicity Evaluation

Cytotoxicity in murine & human cancer cell lines

Derivatives in the **Scheme 1** have been screened towards L1210 cells, CEM cells and HeLa cells to understand their cytotoxicity effect towards all cell lines tested. **Table 1** shows a comparison of the compounds with the anticancer drugs levamisole and melphalan.

10.1002/cbdv.202000800

Table 1. Antiproliferative effects of the compounds on L1210, CEM and HeLa.

Compound	IC_{50}* (μM)		
	CEM	**HeLa**	**L1210**
5a	> 250	> 250	> 250
5b	> 250	> 250	> 250
5c	> 250	> 250	> 250
5d	> 250	> 250	> 250
5e	> 250	> 250	> 250
5f	NT	NT	NT
5g	> 250	> 250	> 250
5h	5.0 ± 3.3	70 ± 4	90 ± 24
6a	> 250	> 250	≥ 250
6b	> 250	> 250	≥ 250
6c	46 ± 9	> 250	2020 ± 68
6d	39 ± 5	46 ± 9	> 250
6e	13 ± 7	18 ± 0	33 ± 10
7a	8.8 ± 2.4	17 ± 0	42 ± 19
7b	28 ± 2	23 ± 0	59 ± 29
7c	61 ± 6	21 ± 5	87 ± 20
7d	59 ± 14	20 ± 3	100 ± 15
7e	11 ± 7	16 ± 5	65 ± 41
7f	84 ± 31	63 ± 13	58 ± 40
7g	0.79 ± 0.35	0.78 ± 0.13	1.6 ± 0.2
8a	> 250	96 ± 24	> 250
8b	0.94 ± 0.12	1.3 ± 0.2	1.1 ± 0.2
Melphalan	1.4±0.4	NT	2.13±0.02
Levamisole	>250	>250	206

[*] The values are the mean ± SEM, (n = 3)

In order to evaluate the potential cytotoxic activity of the 22 derivatives of imidazothiadiazoles, we performed a screening using L1210, HeLa and CEM cell lines. Our results showed that compounds in the **5a-h** series were not cytotoxic against all three cell lines tested, except for compound **5h** (IC_{50} 5.0 μM) against human T-lymphocyte CEM cells. Substitution of

bromine atom at the 5th position of the imidazothiadiazole fused moiety gave 5-bromo derivative **6a-e**. Among these bromo derivatives, namely **6d** and **6e** (IC_{50} 13 to 46 μM) were moderate cytotoxic to cell lines. The thiocyanate substitution at the C_5 position of imidazo[2,1-*b*][1,3,4]thiadiazole formed 5-thiocyanato derivatives like **7a-g**, and there was much improvement in cytotoxicity towards all three cells. Among them, compound **7g** (IC_{50} 0.78 – 1.6 μM) emerged as the one with the most potent cytotoxic activity as it was twice more potent. Introduction of formyl (-CHO) group was done at C_5 position of imidazothiadiazole fused ring by Vilsmeier-Haack reaction to get compounds **8a** and **8b** in good yield. Among these formyl series, compound **8b** (IC_{50} 0.94 – 1.3 micromoles) was twice more potent than the standard control compound against all the cell lines tested. In general, 5-thiocyanate and 5-formyl derivatives were more potent in comparison to the control levamisole.

To study the structure-activity relationship on 2-(4-methoxybenzyl)-imidazo[2,1-*b*][1,3,4]thiadiazole ring, substitutions at the C_5 by bromine, thiocyanate, formyl and at C_6 by phenyl/ substituted phenyl and coumarin-3-yl groups have been taken. Presence of bromine at C_5 of imidazothiadiazole fused ring failed to produce any activity, exception with **5h**. It has IC_{50} value of 5 μM against CEM cells with the coumarin-3-yl moiety at C_6 position. By introducing the thiocyanate group at C5, most of these thiocyanate derivatives became moderate to good cytotoxic derivatives 0.78-100 μM. Among these, compound **7g** with coumarin-3-yl became most promising with IC_{50} of 0.78 μM, 0.79 μM and 1.6 μM for HeLa, CEM and L1210 respectively. Introduction of the -CHO substituent and coumarin-3-yl at 5th and 6th position of fused imidazothiadiazole ring produced good activity for **8b** with IC_{50} 0.94 μM, 1.1 μM and 1.3 μM for CEM, L1210 and HeLa, respectively.

The most potent compounds namely **7g** and **8b** were studied further against Jurkat (Acute T Cell Leukemia), CCRF-CEM (Acute Lymphoblastic leukemia), and Hs27 (Non-cancerous fibroblast) as described below.

Compound 7g is selective towards leukemia cells compared to non-cancer cells

We examined the cytotoxic activity of compounds **7g** and **8b** in an additional leukemia cell line. For this, we used the Jurkat human cell line, which is derived from a patient with Acute T Cell Leukemia. The cytotoxic activity of compounds **7g** and **8b** was evaluated by using differential nuclear staining (DNS) assay.[25] Different concentrations of the compounds were used to calculate the concentration at which the compound is causing the death of 50% of the cell population. Vehicle (DMSO), H_2O_2 and the untreated control samples were also included. As expected, our results indicate that compounds **7g** and **8b** exhibit cytotoxic effects against the Jurkat cell line and the CC_{50} ranged from 1.65 μM to 4.73 μM. Compound **8b** exerted more cytotoxic effect as shown in **Table 2**. We then evaluated the selectivity of these compounds towards cancer cells by analyzing their cytotoxic effect in the Hs27, a non-cancerous fibroblast cells. The CC_{50} obtained from the leukemia cells (Jurkat and CEM) was compared to the noncancer cell line (Hs27) to calculate the selectivity of the compounds towards cancer cells. The compound **7g** exhibited tumor-selective cytotoxicity showing high selectivity index (SCI) values on the Jurkat and CEM cell lines. Whereas the compound **8b** did not exhibit selectivity towards cancer cells. The Jurkat cell line was selected for further experimentation due to its low CC_{50}values with higher SCI.

Table 2. Concentration at which the compounds **7g** and **8b** causes the death of 50% of the leukemia cells (Jurkat and CEM) as well as the human fibroblast cell line (Hs27). This table depicts the selectivity index (SCI) of the compounds **7g** and **8b** towards cancer cells vs. noncancer human fibroblast cells (Hs27).

Compound	Cell line	CC50[a]	SCI
7g	**CEM**	4.73±0.22	6.65
	Jurkat	2.36±0.10	13.33
	Hs27	31.45±0.74	
8b	**CEM**	3.62±0.26	0.65
	Jurkat	1.65±0.19	1.43
	Hs27	2.36±0.03	

[a] The CC50 was calculated by normalizing to our DMSO control average cell count and using a linear interpolation equation to determine the CC50. Data are mean ± standard deviation S.D. (n=3)

Compound 7g causes cell death by inducing apoptosis

We used Jurkat cells to further investigate the mechanism of action of compound **7g** because this cell line exhibits the lowest CC_{50} and higher selectivity index. Under normal conditions, phosphatidylserine is localized in the inner side of the cell membrane. However, during apoptosis, the cell membrane becomes compromised causing externalization of phosphatidylserine. [26,27] We examined the levels of phosphatidylserine externalization in cells treated with this compound. To measure the levels of phosphatidylserine externalization we used the Annexin V-FITC assay. Annexin V binds phosphatidylserine with high affinity and in this way, the levels of phosphatidylserine externalization can be measured. For this experiment, two concentrations of compound 7g were used CC_{50} (2.36 μM) and the CC_{100} (4.72 μM). Our results indicate that this compound is inducing phosphatidylserine externalization in a dose-response manner, as compared to the vehicle control **Figure 2.A.** This result suggests that compound **7g** is causing phosphatidylserine externalization, which is a hallmark of the apoptotic pathway.

Compound 7g does not induce mitochondrial depolarization

Multiple apoptotic pathways can be initiated leading to cell death. One of them is intrinsic apoptotic pathway that can be induced through the loss of mitochondrial transmembrane potential.[28] We investigated the mitochondrial membrane potential of Jurkat cells treated with compound **7g**. For this experiment, we used the JC-1 polychromatic fluorescent reagent. JC-1 is a dye that in cells with normal mitochondrial potential produces red fluorescent J-aggregates by its accumulation in the energized and negatively charged mitochondria. In unhealthy or apoptotic cells this dye also enters the cells but to a lesser degree due to the reduction in negative charge that is caused by the increased membrane permeability. Under these

10.1002/cbdv.202000800

conditions, there is a loss of electrochemical potential that does not allow JC-1 to concentrate and form J aggregates, therefore, JC-1 remains in its original green color. Using flow cytometry we were able to observe that compound **7g** is not causing mitochondrial membrane depolarization. **Figure 2.B**

Compound 7g induces Caspase-3 activation

Another apoptotic pathway that leads to cell death involves the activation of Caspase-3, which the cleavage of multiple proteins that include, PARP-1, CAD, and others.[28] To extend the findings that compound **7g** induces apoptosis, the activation of Caspase-3 was measured in Jurkat cells treated with the compound **7g** CC_{50} (2.36 μM) and CC_{100} (4.72 μM) concentrations, vehicle (DMSO) and untreated control for 7hrs. For this experiment, the NucView caspase-3 substrate was used and the cells were analyzed using flow cytometry. Our results indicate that compound **7g** induced statistically significant activation of caspase-3 when compared to the controls (**Figure 2.C).** These findings provide further evidence to support that compound **7g** induces cell death via apoptotic events.

10.1002/cbdv.202000800

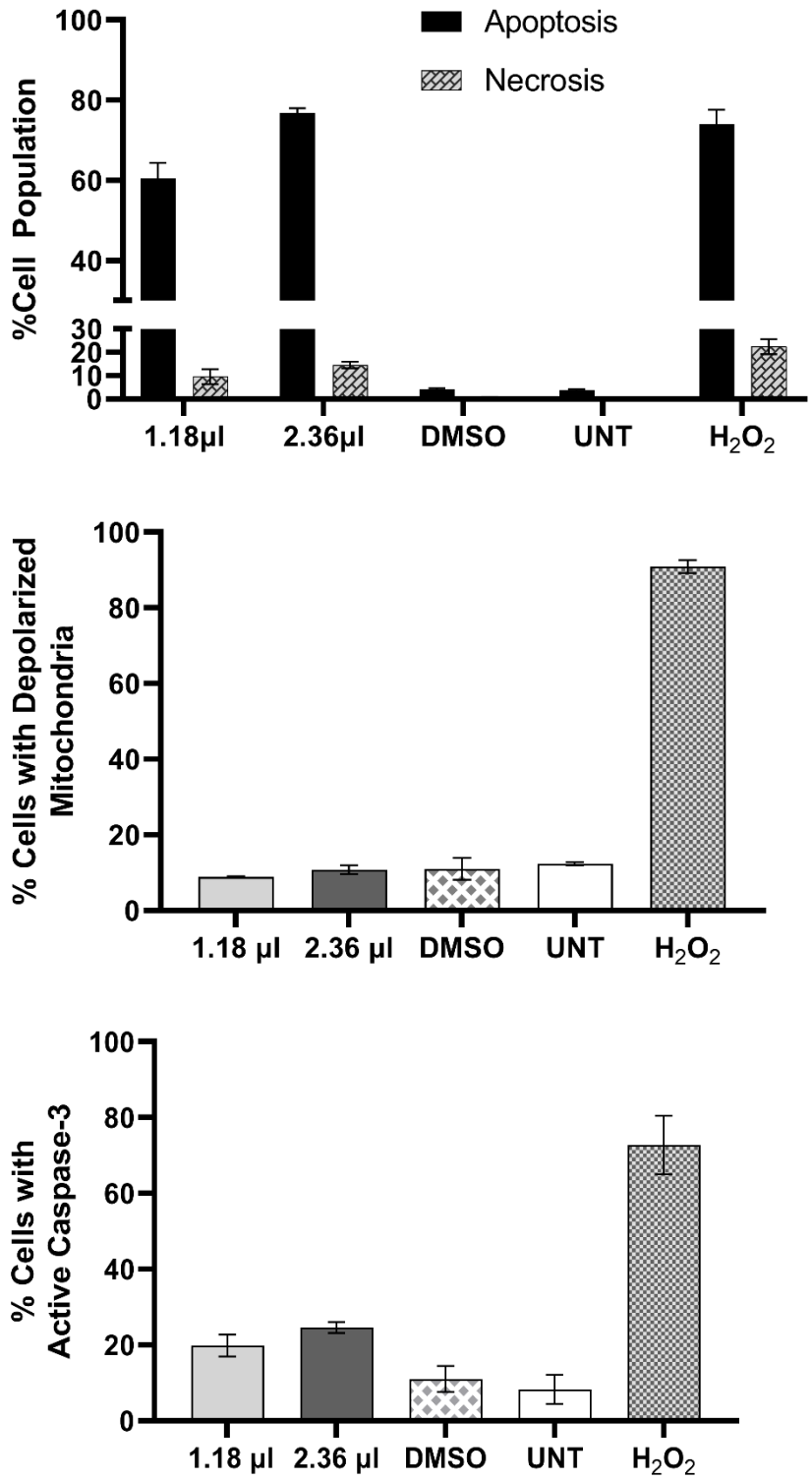

Figure 2 A. Annexin-V-FITC was used to detect phosphatidylserine externalization after treatment with compound **7g**. Results indicate that the compound induces phosphatidylserine externalization which is a biochemical hallmark of apoptosis. **B.** Compound **7g** mediated cytotoxicity does not induce mitochondrial ΔΨm depolarization in Jurkat cells. **C.** Compound **7g** treatment induces caspase-3 activation. Data are mean ± standard deviation S.D. (n=3) *P-value<0.05

10.1002/cbdv.202000800

Compound 7g prevents DNA synthesis and cytokinesis

In order to have a better understanding of the effect of compound **7g** on cancer cells, we decided to perform a cell cycle analysis on Jurkat cells treated with this compound. The cell cycle profile of Jurkat cells was examined *via* flow cytometry utilizing the DNA intercalating agent, DAPI (4',6-diamidino-2-phenylindole). Jurkat cells were exposed to the compound **7g** CC_{50} (2.36 μM) and CC_{100} (4.72 μM) concentrations and incubated for 48 hours and subsequently treated with a nuclear isolation medium (NIM) containing DAPI as previously described.[29] Cytometric analysis of cell cycle progression was performed to investigate if the DAPI fluorescent signal of each treatment. It was measured to quantify the DNA content in the different samples. A vehicle (DMSO) and an untreated control were added. An increase in DNA fragmentation was found in cells treated with 7g which was indicated by an increase in sub-G0 / G1 subpopulation **Figure 3.C**. Interestingly, we observed a decrease of cell subpopulation in the G0-G1 phase and an increase of cell population in the S phase on the cells treated with the CC_{50} **Figure 3.C** An additional increase of the cell population in the G2-M phase can be observed as well.

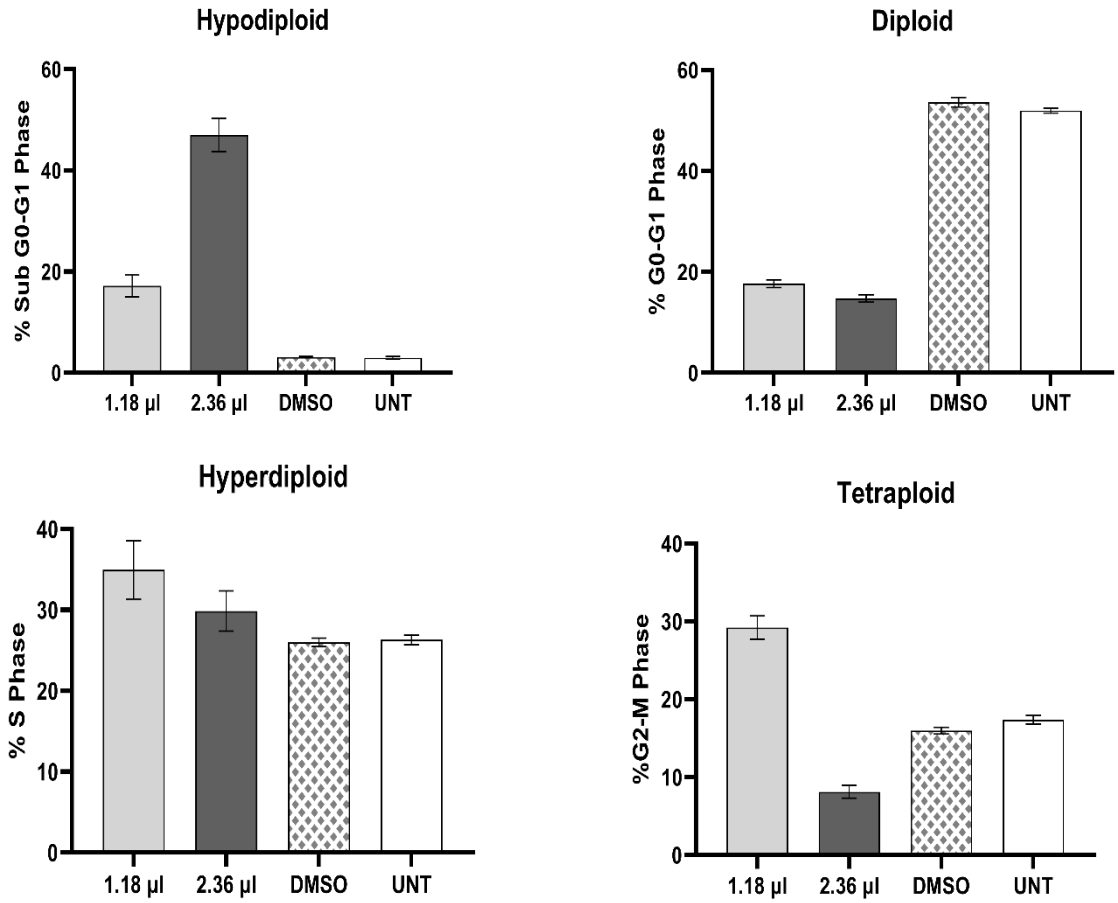

Figure 3. Cell cycle analysis of Jurkat cells treated with compound **7g**. **A**. Increase in the sub-G0-G1 phase subpopulation on the cells treated with the compound's CC_{50}. **B**. Decrease of the cell population in the G0-G1 phase on the cells treated with the compound's CC_{50}. **C**. The increase of cell population can be identified in the S phase on the cells treated with the compound's CC_{50}. **D**. The increase of the cell population in the G2-M phase can be observed on the cells treated with the compound's CC_{50}. Data are mean ± standard deviation S.D. (n=3) *P-value<0.05

In silico analysis

Molecular docking studies

Increased expression of TGF β receptor kinase *I* is an important hallmark of malignant cancer.[30,31] In the present study, molecular docking of two potent synthesized compounds **7g** and **8b** were docked against the active site of TGF β receptor kinase *I* using Glide module. Co-crystallized ligand i.e. heteroaryl substituted 5,6-dihydro-4H-pyrrolo[1,2-*b*]pyrazole in this protein (PDB: 1RW8) was used as a reference molecule in our docking simulations. The root

10.1002/cbdv.202000800

mean square deviation (RMSD) between the docked and co-crystallized ligand was 0.273 Å, suggesting that our docking protocol was accurate to test the newly synthesized molecule**s.** Docking of the well-known compound Melphalan was also performed to reveal its interaction with this kinase target. Details of the Glide docking score and interacting residues are depicted in **Table 3**. **Figure 4** shows the molecular mechanism of interaction between (a) **7g** (b) 3-(4-fluorophenyl)-2-(6-methylpyridin-2-yl)-5,6-dihydro-4H-pyrrolo[1,2-*b*] pyrazole and (c) melphalan with the TGF β type I receptor kinase domain. The most potent *in vitro* molecule **7g** showed best docking score (binding affinity) in comparison to 5,6-dihydro-4H-pyrrolo[1,2-b] pyrazole derivative as depicted in **Table 3**. The potent molecule **7g** made strong hydrogen bonding with S280 and Y282, hydrophobic interaction with A230, K232, L260, V219, A350, L340 and I211 residues, which is in good agreement with the 3-(4-fluorophenyl)-2-(6-methylpyridin-2-yl)-5,6-dihydro-4*H*-pyrrolo[1,2-b] pyrazole binding site residues of kinase I receptor domain (**Table 3**)[32] Melphalan and molecule **8b** showed moderate binding affinities and hydrogen bonding interactions with the kinase active site residues (**Table 3, Figure 4**).

10.1002/cbdv.202000800

Table 3. Interaction details between TGF β type I receptor kinase domain and potent molecules using Glide docking technique.

Molecule	XPGlide score (kcal/mol)	Molecular interactions towards TGF β type I receptor kinase domain				
		Hydrogen bond	Hydrophobic interactions			Other
7g	-7.012	S280 Y282	A230 V219 I211	K232 A350	L260 L340	--
8b	-4.864	K232 S280 G212	V219 A230 K213	K232 L260	L278 L340	D290 (Electrostatic)
[a]3-(4-fluorophenyl)-2-(6-methylpyridin-2-yl)-5,6-dihydro-4H-pyrrolo[1,2-b]pyrazole	-8.784	H283 Y282 D351	L260 V219 A230	L278 K232 L340	Y249 A350	H283 (Halogen)
Melphalan	-5.291	I211 E284 S280	A230 L340	K232	V219	L278 (Halogen)

[a]Reference molecule used in Glide docking.

10.1002/cbdv.202000800

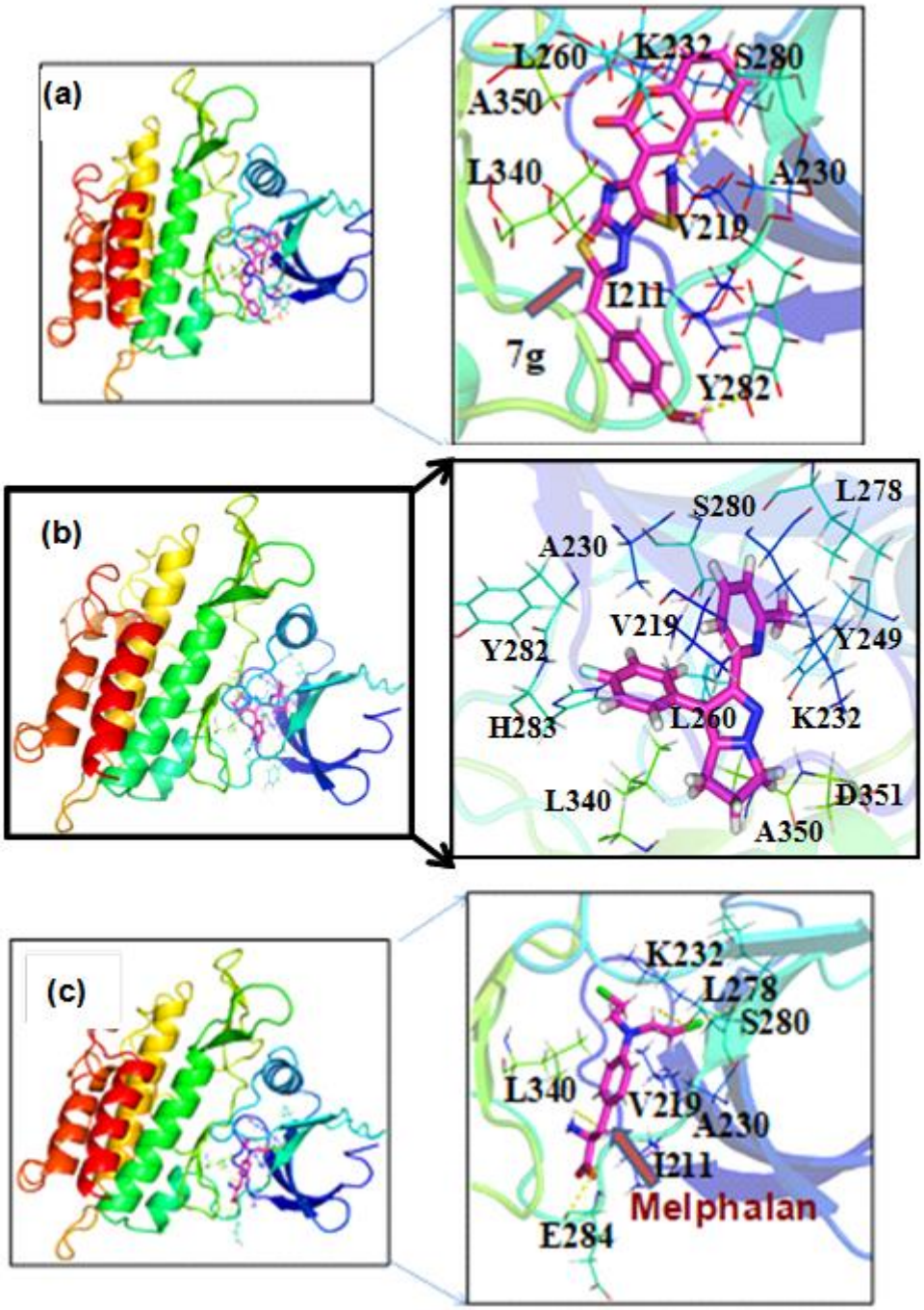

Figure 4. Molecular interactions between TGF beta kinase I receptor with the (**a**) most potent synthesized molecule **7g** (**b**) co-crystallized ligand 3-(4-fluorophenyl)-2-(6-methylpyridin-2-yl)-5,6-dihydro-4H-pyrrolo[1,2-b]pyrazole and (**c**) Melphalan using Glide docking technique. The molecular interaction figures are reproduced using PyMol software.

Discussion

In this study, we synthesized 22 variants of 2-(4-methoxybenzyl)-6-substituted-imidazo[2,1-*b*][1,3,4]-thiadiazole that were expected to have cytotoxic activity against leukemia. Our results indicate that compound **7g** exhibits potent cytotoxicity on one murine

leukemia cells and two human leukemia cancer cells. In addition, compound **7g** exhibited favorable selective cytotoxicity towards leukemia cells when compared to the Hs27 non-cancerous fibroblast cells. We investigated the mechanism of action of compound **7g** by performing different assays. First, we evaluated if the compound was causing cell death by inducing the apoptotic pathway by using the Annexin V-FITC-PI assay. Our results indicate that the compound induces high levels of phosphatidylserine externalization. Furthermore, we investigated the effect of compound **7g** in Jurkat cell membrane potential. We found that compound **7g** does not induce mitochondrial depolarization by the absence of JC-1 dimerization compared to the controls. Caspase-3 activation was analyzed, and our findings show strong caspase-3 activation upon compound **7g** treatment, suggesting that compound **7g** activates the intrinsic apoptotic pathway. To further understand the effect of compound **7g** in leukemia cells, we performed cell cycle analysis. We observed an increase of the sub-G0-G1 phase that represents the subpopulation with DNA fragmentation. Moreover, results show a decrease in the G0-G1 phase with an increase in the S and G2/M phases, where DNA is synthesized, and cytokinesis occurs respectively. Together, our cycle analysis assay suggests that the compound is preventing the cells from proceeding from the S phase by affecting DNA synthesis. The high population of cells in the G2-M phase suggests that the compound could be blocking cytokinesis that is the last step during cell replication. Molecular docking analysis showed that compound **7g** has better binding affinity in comparison to **8b** and Melphalan. **7g,** the most potent synthesized compound also made hydrogen bonding and other week interactions at the active sites of TGF β receptor kinase I domain as explained above (**Figure 4a**). Anti-cancer activity and selectivity of compounds **7g** and **8b** clearly shown that **7g** exhibited high SCI in different cancer cell lines by preventing DNA synthesis and cytokinesis, that could be further correlated with the higher binding affinity of this molecule (-7.012 kcal/mol) obtained from our docking simulations, as shown in **Table 3**. Further, SAR studies

presumes that the good cytotoxicity of **7g** molecule might be due to the presence of SCN substituent at 5th position of fused imidazothiadiazole nucleus and that contributed in better interaction at the active sites of the TGF β receptor kinase I resulting in high binding affinity (**Table 3** and **Figure 4a**). Thus, the present integrated SAR study discovered a novel molecule **7g** showing potent anti-cancer activity for the treatment of leukemia.

Conclusions

22 compounds with different substitution on imidazothiadiazoles fused ring were prepared, characterized by $^{1}H/^{13}C$-NMR, HR-MS and FTIR. All these derivatives tested for cytotoxic activity against a murine leukemia cell line and two human leukemia cell lines. SAR study displayed that the presence of -SCN and -CHO on the 5th position of imidazothiadiazole displayed moderate to good cytotoxicity. Overall, **7g** and **8b** resulted to be more toxic to the cell lines tested. Therefore, these two compounds were further screened using the leukemia cell line Jurkat, and the non-cancer human fibroblast cell line Hs27. Compound **7g** but not **8b** showed favorable selective cytotoxic activity against leukemia cells compared to the human non-cancer fibroblast cells (Hs27). Compound **7g** induces high levels of phosphatidylserine externalization and caspase-3 activation in the Jurkat cell line. These results confirm that the compound is inducing cell death in the Jurkat cell line by initiating the apoptotic pathway. Our cell cycle analysis suggests that the compound interferes with DNA synthesis denoted by the increase of cell population in the S-Phase. The cell population increase in the G2-M phase suggests that the compound is inhibits cytokinesis. Furthermore, molecular docking showed that **7g** binds within the active site of TGF β type I receptor kinase domain by strong hydrogen bonding and hydrophobic interactions. Our results identify compound **7g** as a novel potential anti-leukemia compound. Further studies should be performed to evaluate the effect of this compound in xenograft mouse models.

10.1002/cbdv.202000800

Experimental Section

Chemicals and reagents

Jasco 430+ instrument was used for recording FTIR spectra in KBr by using diffuse reflectance technique; the $^{1}H/^{13}C$ NMR spectrum was taken in $CDCl_3$/ DMSO-d_6 on a Jeol JNM-ECZ400S/ Bruker (400 MHz). XEVO G2-XS QTOF Mass Spectrometer was used to report HR-MS. 2-bromoacetophenone,[33] 2-bromo-4'-chloroacetophenone,[34] 2,4'-dibromoacetophenone,[35] 2-bromo-4'-methoxyacetophenone,[36] 2-bromo-4'-methylacetophenone,[37] 2-bromo-4'-fluoroacetophenone,[38] 2-bromo-4'-nitroacetophenone,[39] 3-(bromoacetyl)coumarin,[40] 2-amino-5-(4'-methoxybenzyl)-1,3,4-thiadiazole **(3)**, compounds **5a**, **5c**, **5d**, **5e**, **5f**, **5g** and **8b** prepared as per literature.[41]

Cell lines and culture conditions

The cell lines used in this study consists of Jurkat (Acute T Cell Leukemia), CCRF-CEM (Acute Lymphoblastic leukemia), and Hs-27 (Non-cancerous fibroblast). The Jurkat and CCRF-CEM cell lines were supplemented with RPMI-1640 medium and an antibiotic mixture of 25µg/ml amphotericin B, 1000 U/ml penicillin, and 1000 µg/ ml streptomycin, and 10% heat-inactivated fetal bovine serum. The Hs-27 cell line was grown in DMEM media with the same additives added to the RPMI media.

Cytotoxicity in human and murine tumor cell lines

The synthesized derivatives have been screened for their cytotoxicity study as per the published procedure.[21] Experiments have been performed in triplicate and the IC50 values were calculated and expressed in micromoles.

Cytotoxic activity in human tumor cell lines

Cytotoxic activity was based on inhibition of HEL cell growth. HEL cells were incorporated into 5 X 10^3 cells / well into 96 microtiter plates and allowed to replicate for 24 h. After that, the medium containing a different concentration of the test compounds was added. After 3 days of incubation at 37 ° C, a cell number was found with the Coulter counter. The cytotoxic concentration was calculated as CC50 (the compound concentration required to reduce cell growth by 50% relative to the number of cells in the untreated controls). CC50 values were estimated from graphic plots of the number of cells (percentage of control) as a function of the concentration of the test compounds. Cytotoxicity was expressed as a minimum cytotoxic concentration (MCC) or the compound concentration that causes a microscopically detectable alteration of cell morphology. All tests were performed and repeated three times.

Differential Nuclear Staining Assay

In order to analyze the potential cytotoxicity of the compounds that were synthesized, the Differential Nuclear Staining Assay (DNS) was used which has been validated for high throughput compound screening.[25] The DNS assay involves the use of two dyes, propidium iodide (PI) and Hoechst. While Hoechst permeates and stains the nuclei of healthy and dead cells, PI can only penetrate and stain nuclei of cells with compromised membranes. The cells with both Hoeschst (blue) and PI staining (red) are recognized and defined as the dead cell population.[25] Before each assay, cell viability was analyzed to ensure that the cells were at least 95% viable using PI staining and flow cytometry. For the initial cytoxicity screening, cells were seeded in a 96-well microplate at a density of 10,000 cells per well in 100μL of media and incubated for 2 h for non-adherent cells and overnight for adherent cells. A concentration gradient of the compounds from 0.1 to 10 μM was tested. The following controls were added

in each experiment: untreated cells, 1% v/v DMSO solvent, and a positive control for cell death of 1mM H_20_2. Each experimental point, as well as the controls, were assessed in triplicate. Furthermore, two incubation times were performed, 48 h for non-adherent cells, and 72 h for adherent cells. Two hours before the end of the incubation period, a mixture of Hoescht and PI (5 μg/mL final concentration) was added to each well, and the plates were incubated for the remaining 2 hours. After incubation, four images were obtained to create a 2x2 montage using a 10X target and two fluorescent channels (Hoechst and PI signals) using the IN Cell Analyzer 2000 system. The images were separated and analyzed in both live and dead cells using software IN Cell Analyzer Workstation 3.2, to determine the percentage of each cell and each source.

Mitochondrial depolarization assay

Cells are grown in a clear 24-plate plate at a density of 200,000 cells / well. After 5 h of compounds treatment, the cells were subjected to cationic polychromatic JC-1 (5 ', 6,6'-tetrachloro-1,1', 3,3'-tetraethylbenzimidazolylcarbocyanine iodide) reagent at 2 μM (MitoProbe; Life Technologies; M34152). When mitochondria are degraded, JC-1 cannot form a compound and remains as a monomer emitting a green fluorescence signal.[42] After incubation with JC-1, the samples were analyzed using flow cytometry (Gallios; Beckman Coulter). Similar controls have been used as in other apoptosis experiments (see above).

Cytotoxic concentration 50% and selective cytotoxicity index values

CC50 has been described as a combined concentration needed to kill 50% of the cell population. To remove the base of the dead cells, the percentage of dead cells found in the DMSO vehicle control was removed from each test sample, and the applied values were used to calculate the CC50. After this, a linear interpolation equation was used to obtain CC50

values.[43,44] Due to the short duration of compound exposure and dose response, cells are exposed to the CC50 and double that compound concentration. The selected cytotoxicity index describes the potential combination of experimental compounds that kill cancer cells that cause minor or insignificant damage to non-cancer cells. SCI values were calculated by separating the CC50 of the non-cancer control cell line by the CC50 of the cancer cell line as described earlier. [29,43,44]

Annexin V-FITC/PI assay

Jurkat cells are propagated in a mass of 100,000 cells / well with 1 ml of cultural media on a 24-well plate in 1 ml medium. After this, the cells were treated with CC50 concentration of 7g for 24 h. Next, cells are collected and marked with PI and annexin V-FITC according to manufacturer's instructions (Beckman Coulter; IM3546). After incubation, the samples were analyzed using flow cytometry (Cytomics FC 500; Beckman Coulter). The same positive and negative controls have been used as in previous sections. About 10,000 events (cells) were detected per sample and analyzed using the CXP (Beckman Coulter) software tool as described earlier. [42]

Mitochondrial membrane potential polychromatic assay

Jurkat cells are grown in a mass of 100,000 cells / well in a clear 24-plate plate. Jurkat cells were treated with CC50 concentrations per compound for 5 h. Thereafter, the cells were subjected to cationic polychromatic JC-1 (5 ′, 6,6'-tetrachloro-1,1 ′, 3,3'-tetraethyl benzimidazolylcarbocyanineiodide) reagent in the final 1 μM (MitoProbe; Life Technologies; (M34152). In cells with a stable mitochondrial membrane, JC-1 dye binds inside the inner mitochondrial membrane causing a transition from green (~ 529 nm) to red (~ 590 nm). As soon as the mitochondria are broken down, JC-1 cannot form a compound and remains as a

monomer emitting green fluorescence signal. [42] After JC-1 contamination, samples were analyzed using flow cytometry (Cytomics FC 500; Beckman Coulter). Similar controls were used as in other experiments for apoptosis (see above).

Caspase- activation assay

Jurkat cells (100,000 cells / well) were seeded in a 24-source plate per 1 ml complete RPMI-1640 medium. Next, the cells were treated for 7 h with CC50 of the composite compound which subsequently found caspase-3 activation using a fluorogenic NucView 488 caspase-3 substrate designed to identify active caspase-3 within live cells (Biotium; 30,029); as described earlier. [42] After cytometry (Cytomics FC 500; Beckman Coulter) green fluorescence signal cells were classified as apoptotic cells with activated caspase 3. The same positive and negative controls as in other apoptosis trials were also used in this series of tests.

Cell cycle analysis

Jurkat cells were placed in a 24-well plate where 100,000 cells combine containing 1 mL of culture media per well. Cells were treated with CC_{25} and CC_{50} compound concentration for a period of 72 h. The controls included in this series of tests were described in previous sections. The cells are then collected in cytometry flow tubes, separated by centrifugation at 262g for 5 minutes and gently regenerated into 100 μL of new media. Thereafter, 200 μL of nuclear isolation medium (NIM) -DAPI solution was added to the cell configuration and immediately analyzed by flow cytometry.[29,45] The NIM-DAPI reagent can locate nuclei of cells that allow the synthesis of DNA content using a FL-9 detector and a 405-nm laser for excitation purposes. This FL-9 detector picks up a fluorescence signal released when DAPI is attached to DNA and leaves a signal when it is attached to RNA. To obtain a well-defined cell cycle distribution profile, 100,000 cells were detected per sample and analyzed with Kaluza Flow Cytometry

Software. Each test point, and their corresponding controls were analyzed simultaneously and tested three times.

Statistical analysis

All values were expressed as mean ± SEM. The intergroup variance between different groups was measured by one-way ANOVA using Graph Pad Prism, version 6.01. Here, the results were considered statistically significant when * $p < 0.05$.

Protein Preparation

The X-ray coordinates of TGF-beta receptor 1 kinase in complex with heteroaryl substituted 5,6-dihydro-4H-pyrrolo[1,2-*b*]pyrazole ligand at a resolution of 2.4 Å was retrieved from protein databank (PDB) with PDB ID 1RW8.[32] The complex was prepared using the Protein Preparation Wizard module of Schrödinger software (Schrödinger, LLC, New York, 2017).[46] Initially, the 3D structure of the protein was pre-processed by assigning bond orders and adding hydrogen atoms. The protein complex was viewed in PyMol software to check for interactions with water. Water molecules that mediate hydrogen bonding interactions between ligand and the receptor were retained after removing the remaining water molecules. Geometry was optimized using the Optimized Potential for Liquid Simulations 2005 (OPLS-2005) force field in order to avoid any structural errors.

Ligand Preparation

7g and **8b** molecular structures were constructed using software ChemBioDraw Ultra version 11.0 and minimized. 3D structure of Melphalan was downloaded from DrugBank database.[47] All three ligands were further prepared using the LigPrep module in Schrödinger software.[48]

3D structure of the ligand was optimized using the OPLS 2005 force field while retaining its specified chirality.

Receptor grid generation

Glide (Grid-based Ligand Docking with Energetics) program of Schrödinger suite was used to generate a receptor grid for docking.[49] The ligand bound to the protein in the complex was picked and a receptor grid was automatically generated by the software around the binding site of the protein. Receptor grids were calculated for prepared proteins such that various ligand poses bind within the active site during docking. Grids were generated keeping the default parameters of van der Waals scaling factor 1.00 and charge cut-off 0.25 subjected to OPLS 2005 force field. A cubic box of specific dimensions 20Å × 20Å × 20Å was generated in the TGF-beta receptor 1 kinase active site for docking simulations.

Molecular Docking

Molecular docking was performed in two stages: The first stage includes SP (standard-precision) docking followed by XP (extra-precision) docking with higher accuracy and less false positives. The Glide XP binding free energy is calculated using the following equation:

$$\text{XP Glide score} = E_{coul} + E_{vdW} + E_{bind} + E_{penalty}$$

Where,E_{coul}, E_{vdW}, and E_{bind} represent the electrostatic potential energy, van der Waals energy, and binding interaction energy respectively. Epenalty is the strain energy from protein, ligand, or both, loss of entropy of the ligand and protein and desolvation of the ligand or protein.[46]The binding interaction of these ligands to the active site of TGF beta receptor kinase was ranked based on the Glide XP scoring function. Hydrogen bonding (H-bonding) and hydrophobic interactions between these complex systems were analyzed by Discovery Studio v19 and PyMol software.

Acknowledgement

Many thanks to NMR Research Centre-Indian Institute of Science, Bengaluru (Karnataka) India for ^{1}H-NMR, Sophisticated Analytical Instrument Facility (SAIF)-Dharwad, (Karnataka) India for ^{13}C-NMR spectroscopy. We sincerely thank facility for HR-MS, Dept. of Chemistry, Indian Institute of Technology, Ropar (Punjab) India. CGM acknowledges Centre for Nanosciences and Molecular Medicine, Amrita Vishwa Vidyapeetham, Kochi for computational infrastructure support. This research was funded by NIH-MARC Program under Grant No. T34GM008048-35 and was performed in facilities funded by the National Institute on Minority Health and Health Disparities (NIMHD) Grant no. 5U54MD007592 to the Border Biomedical Research Center UTEP.

Author contribution statement

C. B. and S. K. Performed the synthetic parts of experiment. D. S. Carried out cytotoxicity study. K. G. C. H. and A. Y. S. B. performed biochemical study. A. M. T. designed and performed the docking study. C. G. M. analyzed and compiled the docking study. S. S. K. and R. J. A. designed the experiment, analyzed spectral and biochemical data, compiled and wrote the paper.

References

[1] American Cancer Society: 'Cancer Facts & Statistics', (n.d.). Retrieved from https://cancerstatisticscenter.cancer.org/

[2] MD;, D. (n.d.). 'Leukemia: An overview for primary care', Retrieved from https://pubmed.ncbi.nlm.nih.gov/24784336/2.

[3] 'What Is Acute Lymphocytic Leukemia (ALL)?: Acute Lymphocytic Leukemia (ALL). (n.d.)', Retrieved from https://www.cancer.org/cancer/acute-lymphocytic-leukemia/about/what-is-all.html

[4] 'What Is Chronic Myeloid Leukemia?: Leukemia Types. (n.d.)', Retrieved from https://www.cancer.org/cancer/chronic-myeloid-leukemia/about/what-is-cml.html

[5] 'Chemotherapy for Acute Lymphocytic Leukemia (ALL). (n.d.)' Retrieved from https://www.cancer.org/cancer/acute-lymphocytic-leukemia/treating/ chemotherapy.html

[6] 'Leukemia - Cancer Stat Facts. (n.d.)', Retrieved from https://seer.cancer.gov/statfacts/html/leuks.html

[7] 'FDA approval: Levamisol', Retrieved from https://www.accessdata.fda.gov/scripts/cder/daf/index.cfm?event=overview.process&ApplNo=020035

[8] K.C. Lee, B. Ladizinski, D.G. Federman, 'Complications associated with use of levamisole contaminated cocaine: an emerging public health challenge', *Mayo Clin. Proc.* **2012**, *87*, 581-586.

[9] N. Scheinfeld, J.D. Rosenberg, J.M. Weinberg, 'Levamisole in dermatology: a review', *Am. J. Clin. Dermatol.* **2004**, *5*, 97-104.

[10] M. Lehtinen, P. Ahrenberg, A. Hänninen, E. Ikkala, R. Lahtinen, A. Levanto, I. Palva, Rajamäki, S. Rosengard, T. Ruutu, S. Sarna, O. Selroos, T. Timonen, E. Waris, C. Wasastjerna, J. Vilpo, P. Vuopio, ,The Finnish leukaemia group: Levamisole in maintenance therapy of acute myeloid leukemia in adults', Retrieved from https://pubmed.ncbi.nlm.nih.gov/6949237/

[11] N. Nakano, Y. Tsuchiya, K. Kako, K. Umezaki, K. Sano, S. Ikeno, E. Otsuka, M. Shigeta, A. Nakagawa, N. Sakata, F. Itoh, Y. Nakano, S.I. Iemura, M.van Dinther, T. Natsume, P.T. Dijke, S. Itoh, 'TMED10 protein interferes with transforming growth factor (TGF)-beta signaling by disrupting TGF-beta receptor complex formation', *J. Biol. Chem.* **2017**, *292*, 4099–4112.

[12] J.M. Yingling, K.L. Blanchard, J.S. Sawyer, 'Development of TGF-beta signaling inhibitors for cancer therapy', *Nat. Rev. Drug Discov.* **2004**, *3*, 1011–1022.

[13] A.C. de Gouville, V. Boullay, G. Krysa, J. Pilot, J . M. Brusq, F. Loriolle, J. M. Gauthier, S.A. Papworth, A. Laroze, F. Gellibert, S. Huet, 'Inhibition of TGF- β signaling by an ALK5 inhibitor protects rats from dimethylnitrosamine- induced liver fibrosis', *Br. J. Pharmacol.* **2005**, *145*, 166–177.

[14] L. Bueno, D.P. de Alwis, C. Pitou, J. Yingling, M. Lahn, S. Glatt, I.F. Trocóniz, 'Semi-mechanistic modelling of the tumour growth inhibitory effects of LY2157299, a new type I receptor TGF-beta kinase antagonist, in mice', *Eur. J. Cancer* **2008**, *44*, 142-150.

[15] H.M. Patel, B. Sing, V. Bhardwaj, M. Palkar, M.S. Shaikh, R. Rane, W. S. Alwan, A. K. Gadad, M.N. Noolvi, R. Karpoormath, 'Design, synthesis and evaluation of small molecule imidazo[2,1-*b*][1,3,4]thiadiazoles as inhibitors of transforming growth factor- β type-I receptor kinase (ALK5)', *Eur. J. Med. Chem.* **2015**, *93*, 599-613.

[16] G. Hoelzemann, H. Greiner, E. Rossignol, D. Swinnen, WO 2010/012345 A1, **2010**.

[17] A.K. Gadad, S.S. Karki, V.G. Rajurkar, B.A. Bhongade, 'Synthesis and biological evaluation of 5-formyl-6-arylimidazo-(2,1-*b*)-1,3,4-thiadiazole-2N-(dimethylaminomethino)-sulfonamides as antitumor agents', *Arzneim.- Forsch./Drug Res.* **1999**, *49*, 858-863.

[18] S.S. Karki, K. Panjamurthy, S. Kumar, M. Nambiar, S.A. Ramareddy, K.K. Chiruvella, S.C. Raghavan, 'Synthesis and biological evaluation of novel 2-aralkyl-5-substituted-6-(4'-

fluorophenyl)-imidazo[2,1-*b*][1,3,4]thiadiazole derivatives as potent anticancer agents,' *Eur. J. Med. Chem.* **2011**, *46*, 2109-2116.

[19] M. Hegde, S.S. Karki, E. Thomas, S. Kumar, K. Panjamurthy, S.R. Ranganatha, K.S. Rangappa, B. Choudhary, S.C. Raghavan, 'Novel levamisole derivative induces extrinsic pathway of apoptosis in cancer cells and inhibits tumor progression in mice', *PLoS ONE* **2012**, *7*, 43632.

[20] S. Kumar, M. Hegde, V. Gopalakrishnan, R.V. Kumar, S.A. Ramareddy, G.N. Anilkumar, E.De Clercq, D. Schols, S.C. Raghavan, S.S. Karki, '2-(4-Chlorobenzyl)-6-arylimidazo[2,1-*b*][1,3,4]thiadiazoles:synthesis, cytotoxic activity and study of mechanism of action,' *Eur. J. Med. Chem.* **2014**, *84*, 687-697.

[21] S. Kumar, V. Gopalakrishnan, M. Hegde, V. Rana, S.S. Dhepe, S.A. Ramareddy, A. Leoni, A. Locatelli, R. Morigi, M. Rambaldi, M. Srivastava, S.C. Raghavan, S.S. Karki. 'Synthesis and antiproliferative activity of imidazo[2,1-*b*][1,3,4]thiadiazole derivatives,' *Bioorg. Med. Chem. Lett.* **2014**, *24*, 4682-4688.

[22] A. Katiyar, B. Metikurki, S. Prafulla, S. Kumar, S. Kushwaha, D. Schols, E.De Clercq, S.S. Karki, 'Synthesis and pharmacological activity of imidazo[2,1-*b*][1,3,4]thiadiazole derivatives,' *Acta Pol. Pharm.* **2016**, *73*, 937-947.

[23] S. Kumar, B. Metikurki, V.S. Bhadauria, E.De Clercq, D. Schols, H. Tokuda, S.S. Karki, 'Synthesis of imidazo[2,1-*b*][1,3,4]thiadiazole derivatives as possible biologically active agents,' *Acta Pol. Pharm.* **2016**, *73*, 913-929.

[24] D. Iyer, S.V. Vartak, M. Hegde, A. Mishra, G. Goldsmith, M. Srivastava, S. Kumar, N. Mayilaadumveettil, M. Glenn, S. Gaikwad, S. Sharma, S. Srivastava, V. Gopalakrishnan, M. Velusamy, B. Choudhary, P. Ray, N. Kalakonda, T. R. Santhosh Kumar, S.S. Karki, Surolia, S.C. Raghavan, 'Identification of a novel BCL2 specific inhibitor that binds predominantly to its BH1 domain', *FEBS Journal* **2016**, *283*, 3408-3437.

[25] C. Lema, A. Varela-Ramirez, R.J. Aguilera, 'Differential nuclear staining assay for high-throughput screening to identify cytotoxic compounds', *Curr. Cell Biochem.* **2011**, *1*, 1-14.

[26] E. Robles-Escajeda, D. Lerma, A.M. Nyakeriga, J.A. Ross, R.A. Kirken , R.J. Aguilera, Varela-Ramirez, 'Searching in mothernature for anti-cancer activity: anti-proliferative and pro-apoptotic effect elicited by green barley on leukemia/lymphoma cells', *PLoS ONE* **2013**, *8*, e73508.

[27] Y. Santiago-Vázquez, U. Das, A. Varela-Ramirez, S.T. Baca, Y. Ayala-Marin, C. Lema, S. Das, A. Baryyan, J.R. Dimmock, R.J. Aguilera, 'Tumor-selective cytotoxicity of a novel pentadiene analogue on human leukemia/lymphoma cells', *Clin. Cancer Drugs* **2016**, *3*, 138–146.

[28] S.W.G. Tait, D.R. Green, 'Mitochondria and cell death: Outer membrane permeabilization and beyond', *Nat. Rev. Mol. Cell Biol.* **2010**, *11*, 621–632.

[29] E. Robles-Escajeda, U. Das, N.M. Ortega, K. Parra, G. Francia, J. R. Dimmock, A. Varela-Ramirez, R.J. Aguilera, 'A novel curcumin-like dienone induces apoptosis in triple negative breast cancer cells', *Cell Oncol.* **2016**, *39*, 265–277.

[30] E.D.G. Fleuren, L. Zhang, J. Wu, R.J. Daly, 'The kinome "at large" in cancer', *Nat. Rev. Cancer* **2016**, *16*, 83–98.

[31] H.N. Abramson, 'The multiple myeloma drug pipeline-2018: A review of small molecules and their therapeutic targets,' *Clin. Lymphoma Myeloma Leuk.* **2018**, *18*, 611-627.

[32] J.S. Sawyer, D.W. Beight, K.S. Britt, B.D. Anderson, R.M. Campbell, T. GoodsonJr, D. K. Herron, H. Li, W.T. McMillen, N. Mort, S. Parsons, E.C.R. Smith, J.R. Wagner, L. Yan, F. Zhang, J.M. Yingling, 'Synthesis and activity of new aryl- and heteroaryl substituted 5,6-dihydro-4*H*-pyrrolo[1,2-*b*] pyrazole inhibitors of the transforming growth factor-β type I receptor kinase domain', *Bioorg. Med. Chem. Lett.* **2004**, *14*, 3581-3584.

[33] A.H. Blatt, Organic Synthesis Coll, vol. 2, John Wiley & Sons, pp. 480.

[34] J. Hartung, M. Schwarz, 'Towards improved alkoxyl radical precursors - the synthesis of N-alkoxy-4-(p-chlorophenyl)thiazole-2(3H)-thiones', *Synlett* **1997**, *7*, 848-850.

[35] T. Ganesh, Ch Harish Kumar, G.L. David Krupadanam, 'A facile synthesis of 2-hydroxy-2-aryl-1,4-benzodioxanes', *Synth. Commun.* **1999**, *29*, 2069-2078.

[36] D.L.J. Clive, S. Hisaindee, D.M. Coltart, 'Derivatized amino acids relevant to native peptide synthesis by chemical ligation and acyl transfer', *J. Org. Chem.* **2003**, *68*, 9247.

[37] M. Ogata, H. Matsumoto, S. Kida, S. Shimizu, K. Tawara, Y. Kawamura, 'Synthesis and antifungal activity of a series of novel 1,2-disubstituted propenones', *J. Med. Chem.* **1987**, *30*, 1497-1502.

[38] S.A. Laufer, D.R.J. Hauser, A.J. Liedtke, 'Regiospecific and highly flexible synthesis of 1,4,5-trisubstituted 2-sulfanylimidazoles from structurally diverse ethanone precursors', *Synthesis* **2008**, *2*, 253-266.

[39] P. Wan, X. Xu, 'Disproportionation of 4-nitroacetophenone to 4-aminoacetophenone and 4-nitrobenzoic acid', *J. Org. Chem.* **1989**, *54*, 4473-4474.

[40] C.F. Koelsch, 'Bromination of 3-acetocoumarin', *J. Am. Chem. Soc.* **1950**, *72*, 2993-2995.

[41] N.P. Badiger, N.S. Shetty, R.S. Lamani, I.A.M. Khazi, 'Synthesis and antimicrobial activitiy of novel barbituric acid and thiohydantoin derivatives of imidazo[2,1-*b*][l,3,4]thiadiazoles', *Heterocycl. Commun.* **2009**, *15*, 433-442.

[42] L. Contreras, R.I. Calderon, A. Varela-Ramirez, H.Y. Zhang, Y. Quan, U. Das, J.R. Dimmock, R. Skouta, R.J. Aguilera, 'Induction of apoptosis via proteasome inhibition in leukemia/lymphoma cells by two potent piperidones', *Cell. Oncol. (Dordrecht),* **2018**, *41*, 623–636.

[43] D.A. Gutierrez, R.E. DeJesus, L. Contreras, I.A. Rodriguez-Palomares, P.J. Villanueva, K.S. Balderrama, L. Monterroza, M. Larragoity, A. Varela-Ramirez, R.J.

Aguilera, 'A new pyridazinone exhibits potent cytotoxicity on human cancer cells via apoptosis and poly-ubiquitinated protein accumulation', *Cell Biol. Toxicol.* **2019**, *35*, 503-519.

[44] A. Varela-Ramirez, M. Costanzo, Y. Carrasco, K. Pannell, R.J. Aguilera, 'Cytotoxic effects of two organotin compounds and their mode of inflicting cell death on four mammalian cancer cells', *Cell Biol. Toxicol.* **2011**, *27*, 159-168.

[45] P.J. Villanueva, A. Martinez, S.T. Baca, R.E. DeJesus, M. Larragoity, L. Contreras, D.A. Gutierrez, A. Varela-Ramirez, R.J. Aguilera 'Pyronaridine exerts potent cytotoxicity on human breast and hematological cancer cells through induction of apoptosis', *PLoS ONE* **2018**, *13*, e0206467.

[46] W.L. Jorgensen, J. Chandrasekhar, J.D. Madura, R.W. Impey, M.L. Klein, 'Comparison of simple potential functions for simulating liquid water', *J. Chem. Phys.* **1983**, *79*, 926–935.

[47] D.S. Wishart, C. Knox, A.C. Guo, D. Cheng, S. Shrivastava, D. Tzur, B. Gautam, M. Hassanali, 'DrugBank: a knowledgebase for drugs, drug actions and drug targets', *Nucleic Acids Res.* **2008**, *36*, D901–906.

[48] R.A. Friesner, J.L. Banks, R.B. Murphy, T. A. Halgren, J.J. Klicic, D.T. Mainz, M.P. Repasky, E.H. Knoll, M.Shelley, J.K. Perry, D.E. Shaw, P. Francis, P.S. Shenkin, 'Glide: a new approach for rapid, accurate docking and scoring. 1. Method and assessment of docking accuracy', *J. Med. Chem.* **2004**, *47*, 1739–1749.

[49] R.A. Friesner, J.L. Banks, R.B. Murphy, T.A. Halgren, J.J. Klicic, D.T. Mainz, M.P. Repasky, E.H. Knoll, M.Shelley, J.K. Perry, D.E. Shaw, P. Francis, P.S. Shenkin, 'Extra precision glide: docking and scoring incorporating a model of hydrophobic enclosure for protein-ligand complexes', *J. Med. Chem.* **2006**, *49*, 6177–6196.